

Actin–Fascin Bundle Formation Under Pressure

LEANDRO FORCINITI,¹ GE WANG,² and MUHAMMAD H. ZAMAN^{3,4}

¹Department of Chemical Engineering, The University of Texas at Austin, Austin, TX 78712, USA; ²Department of Physics, The University of Texas at Austin, Austin, TX 78712, USA; ³Department of Biomedical Engineering, The University of Texas at Austin, Austin, TX 78712, USA; and ⁴Institute of Theoretical Chemistry, The University of Texas at Austin, Austin, TX 78712, USA

(Received 26 January 2009; accepted 5 February 2009)

Abstract—Studies of the dependence of fascin:actin bundle formation on thermodynamic properties are important for understanding cell processes such as migration and differentiation. We report a novel approach utilizing an expanded equilibrium polymerization Flory–Huggins type model to model fascin:actin bundle formation under thermodynamic pressure. A free energy expression that considers both polymer solution physics and both the deactivation of fascin and propagation of fascin:actin bundles was derived for this system. Using this free energy expression, we report the composition's dependency on pressure while varying: fascin to actin molar ratios [1,3, and 6], initial F-actin concentration [9.52×10^{-9} – 5.7×10^{-8} mM], specific volume, and K_{deact} . Bundle formation was shown to increase as a function of pressure and to be limited by F-actin. Furthermore, our model was able to quantitatively predict an optimal size parameter for the deactivated fascin molecule ($s_F = 4645$) and for the deactivation equilibrium constant ($K_{\text{deact}} = 2.66 \times 10^8$). These results present a novel approach to study fascin cross-linking of actin bundles and provide avenues for future experiments to develop a more comprehensive understanding of cell–matrix interactions.

Keywords—Actin, Fascin, Cross-linking, Flory–Huggins.

INTRODUCTION

Filopodia are highly dynamic structures that extend from the lamellipodia of migrating cells.^{13,20} The cytoskeletal composition of filopodia consists of F-actin polymers cross-linked into bundle like morphology through fascin.^{1,23,29,32} Fascin is a small, 55 kDa, protein that has both a protein kinase C and actin binding domain and is deactivated upon phosphorylation of the serine 39 residue.²⁶ In addition to

migration dynamics, it is believed filopodial dynamics determine axon branching¹⁸ and guidance.⁴ A number of studies have shown that topographical cues promote axogenesis, the formation of axon in neurons, and axon guidance,^{6–8,14,19,28,27} which have been studied through both experimental and computational methods.¹⁵ Many hypothesize that this cellular behavior is due to differences in tensile forces seen by the filopodia. These forces are seen by the migrating cell through the assembly and disassembly of focal contacts.^{5,16} Focal contacts provide a mechano-sensory capability to the cell by linking membrane bound integrins with cytoskeletal components such as actin filaments.^{16,17}

Recent studies have shown that filopodia length determined experimentally can be modeled as a good first order approximation using simple mechanical arguments.²² These arguments are based on the mechanics of actin and fascin cross-linked bundles. Stewman and Dinner³⁰ have used a lattice model with Potts-like spins in combination with a Kinetic Monte Carlo algorithm to understand the dynamics of actin self assembly into filopodia like bundles. However, pressure effects of the equilibrium polymerization of both actin and fascin cross-links have never been addressed adequately. In order to develop a better understanding of filopodia mechanics, structure and dynamics, we have developed a computational approach based upon the Flory–Huggins model first developed by Dudowicz *et al.*^{9–12} Previous extensions of this theory have been extended to study actin growth under pressure,^{3,24} however the role of fascin, or the self assembly of these polymer chains into filopodia like bundles through fascin cross-linking has never been addressed. In this work, an extended Flory–Huggins model is used to determine actin and fascin equilibrium polymerization under thermodynamic pressure. Understanding bundle formation under pressure may help develop second generation models describing how cells interact with their substrates and specifically how cells interact with topographical cues on those substrates.

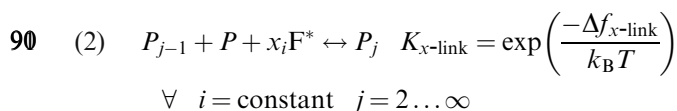
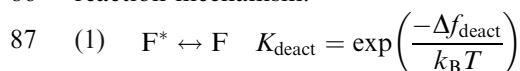
Address correspondence to Muhammad H. Zaman, Department of Biomedical Engineering, The University of Texas at Austin, Austin, TX 78712, USA. Electronic mail: mhzaman@mail.utexas.edu

Leandro Forciniti and Ge Wang contributed equally to this work.

84

MODEL DEVELOPMENT

85 Our model is based on the following simplified
86 reaction mechanism:



95

96

97

98

99

100

101

102

103

104

105

106

107

108

109

110

111

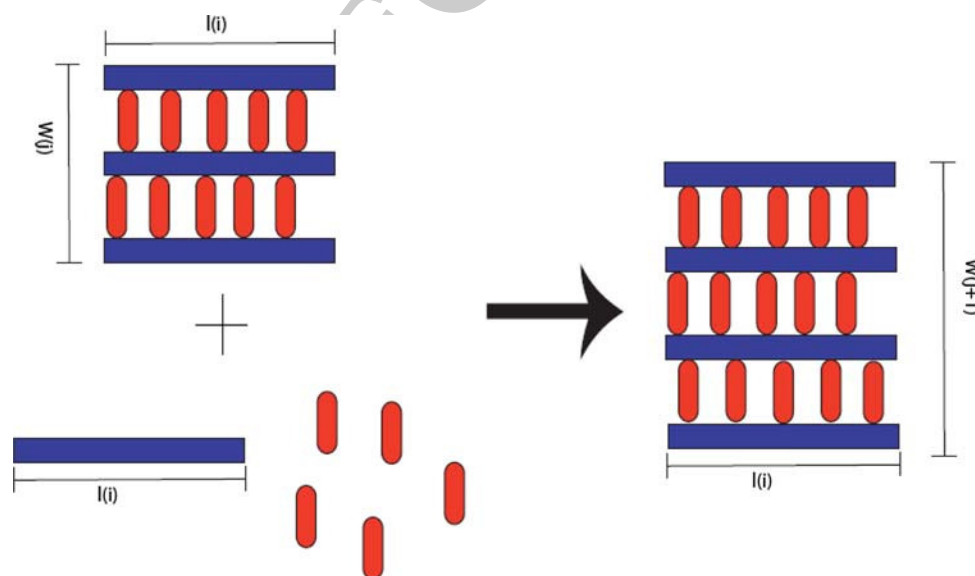
In the above reaction mechanism, reaction (1) describes the deactivation of active fascin through the phosphorylation of the ser39 amino acid. The formation of F-actin fascin polymer networks is described in Eq. (2). For simplicity sake several assumptions were made. First it was assumed that all actin present in our system was fully reacted F-actin polymer with the same extent polymerization. As reported by Tseng *et al.*,³¹ F-actin has an extent of polymerization ranging from 119 to 255 actin monomer units. The effect of bundle of formation was investigated for F-actin polymers that had an extent of polymerization within this range. For simplicity it is assumed that the growth of a bundle network occurs only sequentially and that the number of fascin cross-links between each polymer strand is a constant depending on the extent of polymerization, i , of the F-actin polymer filaments. A schematic of how

112 we propose actin bundles form from fascin:actin net-
113 works can be seen in Fig. 1.

114 In reaction (2), x_i denotes the average degree of
115 cross-linking between F-actin polymers composed of i
116 actin monomers or stated another way x_i is the average
117 number of cross-links per F-actin strand. As a simple
118 approximation it was assumed that this degree of cross-
119 linking had a linear dependency on the degree of
120 polymerization of the actin polymer (i.e., on i). This
121 linear dependency on the degree of polymerization is
122 supported from previous studies reported in literature.¹
123 Aratyn *et al.* observed that in filipodia is one fascin
124 cross-link for every 25–60 actin monomers. This linear
125 dependency can be represented in an equation as:

$$x_i = mi \quad (1)$$

128 In order to determine the slope of this linear equation
129 we considered actin filaments to be hexagonally packed
130 in the bundles. As a consequence, every second mono-
131 mer in the helix would be aligned with an adjacent fil-
132 ament and accommodate a cross-link. In the upper
133 limit, where every available site has a cross-link, this
134 would lead to a fascin:actin ratio, “ m ,” equal to $1/4$. Next
135 we develop our modified Flory–Huggins model by
136 starting with a simple cubic lattice with N sites ($z = 6$).
137 We consider the total number of lattice sites available in
138 our system to be composed of two components: the
139 number of species in our system and the size each species



FIGUER 1. Bundle formation from actin and fascin precursors. The schematic above shows how we visualize fascin:actin bundles forming from bundles, actin, and fascin precursors. For all calculations the number of fascin cross-links per actin monomer was kept at theoretical upper limit ($m = 1/4$) and the extent of polymerization i was kept constant. In the above figure $l(i)$ and $W(j)$ correspond to the extent of polymerization (255) of each F-actin polymer and the extent of polymerization for the bundles. In all simulations the parameters that were kept constant were: $T = 293$, $S_p = 2320$, $\chi_{SP} = -3933.5/T$, and $\chi_{SS} = 1200/T$.

140 takes up vs. a reference. We then write the total number
141 of lattice sites, N_T , to be equal to:

$$N_T = s_s n_s + s_v n_v + s_{F^*} n_{F^*} + s_F n_F + s_p n_p + \sum_{j=2}^{\infty} j (s_{p^*} + x_i s_{x\text{-link}}) n_j \quad (2)$$

143 In Eq. (2), n_s , n_v , n_F , n_{F^*} , n_p , n_j are the corre-
145 sponding number of solvent, vacuum, deactivated
146 fascin, activated fascin, unreacted F-actin poly-
147 mer, and number of bundles composed of j F-actin

In Eq. (3), ϕ_{F^*} , ϕ_F , and ϕ_p are the lattice volume
fractions for activated fascin, deactivated fascin, and
unreacted F-actin polymer, respectively. The last term
in Eq. (3), ϕ_j , is the lattice volume fraction for the
bundle composed of j actin polymers. The size of each
unit in the bundle is a linear combination of the sizes
of the reacted actin polymers, s_{p^*} , and the x_i reacted
fascin cross-links, $s_{x\text{-link}}$.

Following a similar theoretical construct as the
equilibrium polymerization fluid lattice model^{3,2} we
develop a Helmholtz free energy equal to:

$$\begin{aligned} \frac{F}{N_T k_B T} = & f_{\text{salt}} + \frac{\phi_s}{s_s} \ln \phi_s + \frac{\phi_p}{i s_p} \ln \phi_p + \sum_{j=2}^{\infty} \frac{\phi_j \ln \phi_j}{j (s_{p^*} + x_i s_{x\text{-link}})} + \frac{\phi_F}{s_F} \ln \phi_F + \frac{\phi_{F^*}}{s_{F^*}} \ln \phi_{F^*} + \frac{1}{s_v} (1 - R) \ln(1 - R) \\ & + \frac{\phi_p}{s_p} f_p + \sum_{j=2}^{\infty} \frac{\phi_j}{(s_{p^*} + x_i s_{x\text{-link}})} f_j + \frac{\phi_F}{s_F} f_F + \frac{\phi_s^2}{s_s} \chi_{ss} + \left[\frac{\phi_p}{\sqrt{s_p}} \right]^2 \chi_{pp} \\ & + 2\chi_{Bp} \left[\frac{\sum_{j=2}^{\infty} \phi_j \phi_p}{\sqrt{s_p (s_{p^*} + x_i s_{x\text{-link}})}} + \frac{[\sum_{j=2}^{\infty} \phi_j]^2}{2 (s_{p^*} + x_i s_{x\text{-link}})} \right] + 2\chi_{BF} \left[\frac{\phi_F \sum_{j=2}^{\infty} \phi_j}{\sqrt{s_F (s_{p^*} + x_i s_{x\text{-link}})}} + \frac{\phi_{F^*} \sum_{j=2}^{\infty} \phi_j}{\sqrt{s_{F^*} (s_{p^*} + x_i s_{x\text{-link}})}} \right] \\ & + \chi_{FF} \left[\frac{\phi_F}{\sqrt{s_F}} + \frac{\phi_{F^*}}{\sqrt{s_{F^*}}} \right]^2 2\chi_{sB} \left[\frac{\phi_s \sum_{j=2}^{\infty} \phi_j}{\sqrt{s_s (s_{p^*} + x_i s_{x\text{-link}})}} \right] + 2\chi_{sp} \left[\frac{\phi_s \phi_p}{\sqrt{s_p s_s}} \right] + 2\chi_{sF} \left[\frac{\phi_s \phi_F}{\sqrt{s_s s_F}} + \frac{\phi_s \phi_{F^*}}{\sqrt{s_s s_{F^*}}} \right] \\ R = & \phi_s + \phi_F + \phi_{F^*} + \phi_p + \sum_{j=2}^{\infty} \phi_j \end{aligned} \quad (4)$$

148 polymers in our system respectively. Whereas, s_s , s_v , s_F ,
149 s_{F^*} , s_p , s_{p^*} , and $s_{x\text{-link}}$ are the lattice sites occupied by
150 the aforementioned species with the latter two being
151 summed up in the last term of Eq. (1) to take into
152 consideration size changes between unreacted and re-
153 acted species when incorporated in the bundle. Three
154 of these size parameter, s_F , s_{p^*} , $s_{x\text{-link}}$ corresponding to
155 the lattice sites occupied by deactivated fascin, cross-
156 linked polymer, and cross-linking fascin, respectively,
157 can be changed to better fit experimental data or a
158 higher order model.

159 Next we use this total number of sites to define
160 volume fractions for each of the species involved.
161 These volume fractions are defined as:

$$\begin{aligned} \phi_s &= \frac{s_s n_s}{N_T} \\ \phi_p &= \frac{s_p n_p}{N_T} \\ \phi_{F^*} &= \frac{s_{F^*} n_{F^*}}{N_T} \\ \phi_F &= \frac{s_F n_F}{N_T} \\ \phi_j &= \frac{(s_{p^*} + x_i s_{x\text{-link}}) j n_j}{N_T} \quad \forall j = 2 \dots \infty \end{aligned} \quad (3)$$

In Eq. (4), the first term considers any free energy
contribution small ions may contribute in the overall
free energy. The volume associated with these small
ions is considered negligible and is not explicitly con-
sidered. Finally, considerations for the free energy
changes due to any structural changes in shape for the
species involved in the reactions (i.e., F-actin polymers
and fascin) were neglected. The next six terms follow-
ing, f_{salt} , take into consideration the translational
entropy contribution for each of the distinct species in
our system. Terms seven through ten account for the
dimensionless specific free energy of each species in our
system. The final six terms account for the solvent–
solvent, polymer–polymer, bundle–F-actin, bundle–
deactivated fascin, solvent–bundle, fascin–fascin, and
solvent–polymer Flory-Huggin’s interaction param-
eters. In developing these pair-wise interaction param-
eters it was assumed that for the bundle the interaction
between bundle–bundle and freely diffusing polymer is
the same and the fascin cross-links are not accessible to
interact.

In Eq. (4), the dimensionless specific free energy
of each species was used to calculate the specific
free energy contribution for each species. For the

200 deactivated fascin monomer the dimensionless specific
201 free energy is given by:

$$f_F = \frac{\Delta f_{\text{deact}}}{k_B T} \quad (5)$$

203 Since empty sites are not thermodynamic quantities
205 we can write:

$$f_v = 0 \quad (6)$$

208 We define the free energy of unreacted F-actin poly-
209 mer and activated fascin monomers and solvent mole-
210 cules, (f_P, f_{F^*}, f_S) respectively, to be equal to zero defining
211 the zero entropy state. For the cross-linked bundle, we
212 employ a modification to the Flory–Huggins theory
213 similar to the treatment by Lu and Hentschke²¹ that
214 considers the configurational energy of a bundle with
215 extent of polymerization j and the free energy involved in
216 forming a crosslink between to actin polymers:

$$f_j = \frac{1}{j} \frac{\Delta f_{x\text{-link}}}{k_B T} + \frac{j-1}{j} - \ln(z-1) \quad j \geq 2 \quad (7)$$

219 It should be noted that in Eq. (7), we assume that any
220 swelling of our network is negligible and as such we
221 neglect the elastic entropy of our network due to swelling.

222 The $\Delta f_{x\text{-link}}$ term is the free energy associated with
223 each cross-linking event, and j is the number of F-actin
224 polymers that form the bundle. Finally, the thermal
225 energy term, $k_B T$, is present to account for the thermal
226 energy available in the local environment.

227 We now proceed to our treatment of chemical
228 equilibrium. For each of the proposed reactions we
229 assume that we are at chemical equilibrium. At
230 chemical equilibrium the change in chemical potential
231 must be identically equal to zero and as such we write:

$$d\mu = 0 \quad (8)$$

for each reaction. Therefore, with this simplification in
234 hand we get from reactions (1) and (2) 235

$$\mu_F - \mu_{F^*} = 0 \Rightarrow \mu_{F^*}^* = \mu_F \quad (9)$$

$$\mu_j - (j-1)\mu_P - (j-2)x_i\mu_{F^*} = 0 \quad (10)$$

$$\Rightarrow \mu_j = (j-1)\mu_P + (j-2)x_i\mu_{F^*}$$

Combining the definition of chemical potential with
our definition for lattice fractions, we get for our
chemical potentials to be equal to:

$$\begin{aligned} \mu_P &= \frac{s_P i}{N_T} \left(\frac{\partial F}{\partial \phi_P} \right)_{T, N_T, c, n_j \neq i, n_F, n_{x\text{-link}}} \\ \mu_{F^*} &= \frac{s_{F^*}}{N_T} \left(\frac{\partial F}{\partial \phi_{F^*}} \right)_{T, N_T, c, n_j \neq i, n_F, n_{x\text{-link}}} \\ \mu_F &= \frac{s_F}{N_T} \left(\frac{\partial F}{\partial \phi_F} \right)_{T, N_T, c, n_j \neq i, n_F, n_{x\text{-link}}} \end{aligned} \quad (11)$$

$$\mu_j = \left(\frac{s_P^* + x_i s_{x\text{-link}}}{N_T} \right) \left(\frac{\partial F}{\partial \phi_j} \right)_{T, N_T, c, n, n_F}$$

Using these definitions and the free expression
determined in Eq. (4) and solving for the conditions
of chemical equilibrium one can get after some
algebra:

$$\phi_F = \phi_{F^*} e^{\delta F} e^{-\frac{\Delta f_{\text{deact}}}{k_B T}} \quad (12)$$

$$\phi_j = \phi_P^{j-1} \phi_{F^*}^{(j-2)x_i} e^{aj+b} e^{-\frac{j\Delta f_{x\text{-link}}}{k_B T}} \quad (13)$$

$$\begin{aligned} a &= -(s_P^* + x_i s_{x\text{-link}}) \left[2\chi_{BP} \left(\frac{\phi_P}{\sqrt{s_P(s_P^* + x_i s_{x\text{-link}})}} + \frac{\phi_j}{(s_P^* + x_i s_{x\text{-link}})} \right) \right. \\ &\quad \left. + 2\chi_{BF} \left(\frac{\phi_F}{\sqrt{s_F(s_P^* + x_i s_{x\text{-link}})}} + \frac{\phi_{F^*}}{\sqrt{s_{F^*}(s_P^* + x_i s_{x\text{-link}})}} + \frac{2\chi_{SB}\phi_S}{\sqrt{s_S(s_P^* + x_i s_{x\text{-link}})}} \right) \right] \\ &\quad + \frac{(s_P^* + x_i s_{x\text{-link}})}{s_v} (\ln(1-R) + 1) + \ln(z-1) + i s_P \left[\frac{2\chi_{PP}}{s_P} \phi_P + 2\chi_{BP} \left(\frac{\sum_{j=2}^{\infty} \phi_j}{\sqrt{s_P(s_P^* + x_i s_{x\text{-link}})}} \right) + \frac{2\chi_{SP}\phi_S}{\sqrt{s_P s_S}} \right] \\ &\quad + im - \frac{s_{F^*} im (\ln(1-R) + 1)}{s_v} + im s_{F^*} \left[2\chi_{BF} \left(\frac{\sum_{j=2}^{\infty} \phi_j}{\sqrt{s_{F^*}(s_P^* + x_i s_{x\text{-link}})}} \right) + \frac{2\chi_{FF}}{\sqrt{s_{F^*}}} \left(\frac{\phi_F}{\sqrt{s_F}} + \frac{\phi_{F^*}}{\sqrt{s_{F^*}}} \right) 2\chi_{SF} \left(\frac{\phi_S}{\sqrt{s_S s_{F^*}}} \right) \right] \quad (14) \\ b &= \frac{i s_P}{s_v} (\ln(1-R) + 1) - 1 - i s_P \left[\frac{2\chi_{PP}}{s_P} \phi_P + 2\chi_{BP} \left(\frac{\sum_{j=2}^{\infty} \phi_j}{\sqrt{s_P(s_P^* + x_i s_{x\text{-link}})}} \right) + \frac{2\chi_{SP}\phi_S}{\sqrt{s_P s_S}} \right] \\ &\quad - 2im + \frac{2im s_{F^*}}{s_v} [\ln(1-R) + 1] - 2im s_{F^*} \\ &\quad \left[2\chi_{BF} \left(\frac{\sum_{j=2}^{\infty} \phi_j}{\sqrt{s_{F^*}(s_P^* + x_i s_{x\text{-link}})}} \right) + \frac{2\chi_{FF}}{\sqrt{s_{F^*}}} \left(\frac{\phi_F}{\sqrt{s_F}} + \frac{\phi_{F^*}}{\sqrt{s_{F^*}}} \right) 2\chi_{SF} \left(\frac{\phi_S}{\sqrt{s_S s_{F^*}}} \right) \right] \end{aligned}$$

252 In Eqs. (12) and (13), δ_F , a and b are defined as:
 254 A constraint we have in the following expression is
 255 that in order for Eq. (13) to have a closed form overall
 256 for all possible species (i.e., to infinity) the variable “ a ”
 257 must satisfy the following inequality:

$$a < -\ln \phi_p - im \ln \phi_F - \ln K_{x\text{-link}} \quad (15)$$

260 Plugging in the equilibrium constants from our
 261 reactions we get our final expressions for ϕ_j and ϕ_{F^*} :

$$\begin{aligned} \phi_F &= \phi_{F^*} e^{\delta_F} K_{\text{deact}}^F \\ \phi_j &= \phi_p^{j-1} \phi_{F^*}^{(j-2)x_i} e^{aj+b} K_{x\text{-link}}^j \end{aligned} \quad (16)$$

263 With the expression from Eq. (16) we now can
 265 express the actin and fascin species mass conservation
 266 in terms of two variables (ϕ_j and ϕ_{F^*}). Therefore the
 267 mass conservation of actin and fascin is given by:

$$\begin{aligned} \frac{n_{F\text{-actin}}^0}{N_T} &= \frac{\phi_{F\text{-actin}}^0}{i s_p} = \frac{\phi_p}{i s_p} + \left(\frac{1}{s_{p^*} + x_i s_{x\text{-link}}} \right) \\ &\times K_{x\text{-link}}^2 \frac{\phi_p e^{2a+b}}{1 - \phi_p \phi_{F^*}^{x_i} e^a K_{x\text{-link}}} \\ \frac{n_{F\text{-fascin}}^0}{N_T} &= \frac{\phi_{F^*}^0}{s_{F^*}} = \frac{\phi_{F^*}}{s_{F^*}} + \left(\frac{x_i}{s_{p^*} + x_i s_{x\text{-link}}} \right) K_{x\text{-link}}^2 \\ &\times \frac{\phi_p e^{2a+b}}{1 - \phi_p \phi_{F^*}^{x_i} e^a K_{x\text{-link}}} + \frac{\phi_{F^*} K_{\text{deact}} e^{\delta_F}}{s_F} \end{aligned} \quad (17)$$

In Eq. (17), ϕ_{actin}^0 and $\phi_{F^*}^0$ represents the initial concentration of actin and fascin respectively used in the simulation.

Next we add the constraint using the thermodynamic relationship:

$$P = - \left(\frac{\partial F}{\partial V} \right)_{T, n_s, n_i} = - \frac{1}{v_0} \left(\frac{\partial F}{\partial N_T} \right)_{T, n_p, n_{x\text{-link}}, n_s, n_i^*, n_F^*} \quad (18)$$

where v_0 is the volume occupied by one water molecule ($v_0 = 30 \text{ \AA}$). This gives us a relationship that relates the free energy derived in Eq. (5) to thermodynamic pressure.

With Eqs. (16) and (17) we now have three equations with three unknowns (i.e., $\phi_p, \phi_{F^*}, N_T = f(P, T, \phi_{\text{actin}}^0, \phi_{F^*}^0)$).

NUMERICAL METHODS AND PARAMETER ESTIMATION

Several simplifications need to be made to the free energy expression in Eq. (4) before it can be used to solve our system. First, it was assumed that our system is at infinite dilution such that $\phi_s \gg \phi_p \approx \phi_F \approx \phi_{F^*} \approx \phi_j$. In addition, we assume the Flory–Huggins parameters for all species interactions are of the same order of magnitude, therefore, we get that only the solvent interactions are necessary in order to

TABLE 1. Model parameters and their typical values used in this study.

Variable name	Dimension (units)	Physical meaning	Typical value
ϕ_s		The lattice volume fraction for solvent	0.94 (dilute approximation)
$\phi_p, \phi_F, \phi_{F^*}, \phi_j$		The lattice volume fraction for unreacted F-actin, deactivated fascin, activated fascin, the bundle composed of j F-actin filaments	
s_s, s_v	Lattice sites	The lattice sites occupied by solvent molecule, vacuum site	1.0
s_F	Lattice sites	The lattice sites occupied by deactivated fascin	4640
s_{F^*}	Lattice sites	The lattice sites occupied by activated fascin	4580
s_p	Lattice sites	The lattice sites occupied by unreacted F-actin	2320
s_{p^*}	Lattice sites	The lattice sites occupied by F-actin filaments in bundles	i^*2320
$s_{x\text{-link}}$	Lattice sites	The lattice sites occupied by cross-linking fascin	4580
K_{deact}		The deactivation equilibrium constant	2.66×10^8 (default)
$K_{x\text{-link}}$		The cross-linking equilibrium constant	6.7×10^6
l		The number of actin monomers in F-actin	119–255
M		Fascin and actin ratio in bundle	1/4
N_T		The total number of lattice sites	1.0×10^9
$n_s, n_v, n_F, n_{F^*}, n_p, n_j$		The number of solvent molecule, vacuum sites, deactivated fascin, activated fascin, unreacted F-actin, bundles composed of j F-actin filaments	
$[A], [F]$	mM	Initial F-actin and fascin concentration	$9.52 \times 10^{-9}; 1.9 \times 10^{-9}$
$\frac{F}{N_T k_B T}$		Helmholtz free energy normalized by thermal energy	
$\chi_{ss}, \chi_{sB}, \chi_{sp}, \chi_{sF}$		Solvent–solvent, solvent–bundle, solvent–F-actin, solvent–fascin interaction coefficients	Variable
P	Atm	Thermodynamic pressure	1–10
v_0	\AA^3	The volume occupied by one water molecule	30

293 accurately describe our system. This assumption is a
 294 result of the lack of reliable quantitative molecular
 295 level data, theoretical or experimental, on fascin
 296 kinetics and interaction in bundle formation. Based on
 297 these assumptions, we can rewrite Eq. (14) as:

$$\begin{aligned}
 a = & - (s_{P^*} + x_i s_{X\text{-link}}) \left[\frac{2\chi_{SB}\phi_S}{\sqrt{s_S(s_{P^*} + x_i s_{X\text{-link}})}} \right] \\
 & + \frac{(s_{P^*} + x_i s_{X\text{-link}})}{s_V} (\ln(1 - R) + 1) + \ln(z - 1) \\
 & + i_{SP} \left[\frac{2\chi_{SP}\phi_S}{\sqrt{s_{PS}}} \right] + im - \frac{s_{F^*} im (\ln(1 - R) + 1)}{s_V} \\
 & + im s_{F^*} \left[2\chi_{SF} \left(\frac{\phi_S}{\sqrt{s_S s_{F^*}}} \right) \right] \quad (19)
 \end{aligned}$$

$$\begin{aligned}
 b = & \frac{i_{SP}}{s_V} (\ln(1 - R) + 1) - 1 - i_{SP} \left[\frac{2\chi_{SP}\phi_S}{\sqrt{s_{PS}}} \right] - 2im \\
 & + \frac{2im s_{F^*}}{s_V} [\ln(1 - R) + 1] - 2im s_{F^*} \left[2\chi_{SF} \left(\frac{\phi_S}{\sqrt{s_S s_{F^*}}} \right) \right]
 \end{aligned}$$

303 Substituting these simplified expressions into our
 304 mass balance given in Eq. (16) and using Matlab's
 305 fsolve numerical solver, we solve our two variables as a
 306 function of the total number of lattice sites, N_T .
 307 Equation (17) was subsequently solved numerically to
 308 fully determine the composition of our system as a
 309 function of pressure. Due to the complexity of the
 310 system several parameters had to be estimated from
 311 experimental conditions whereas others were deter-
 312 mined to fit the numerical constraints that were
 313 implemented in order to get physically realizable data.

314 We assumed that the volume fraction of actin is
 315 much less than the volume fraction of solvent. This
 316 allows us to safely assume that the number of vacant
 317 sites, n_V , is determined by the solvent only. Therefore,
 318 we define in the numerical algorithm the volume
 319 fraction of vacant sites to be equal to that in the lattice
 320 model of pure water ($R \sim O(10^{-2})$).³ For the solvent-
 321 solvent interaction parameter, χ_{SS} , we determined that
 322 its functionality was equal to that determined previ-
 323 ously from fits to the compressibility of pure water
 324 over the pressures of interest (i.e., $\chi_{SS} = 1200/T$ for

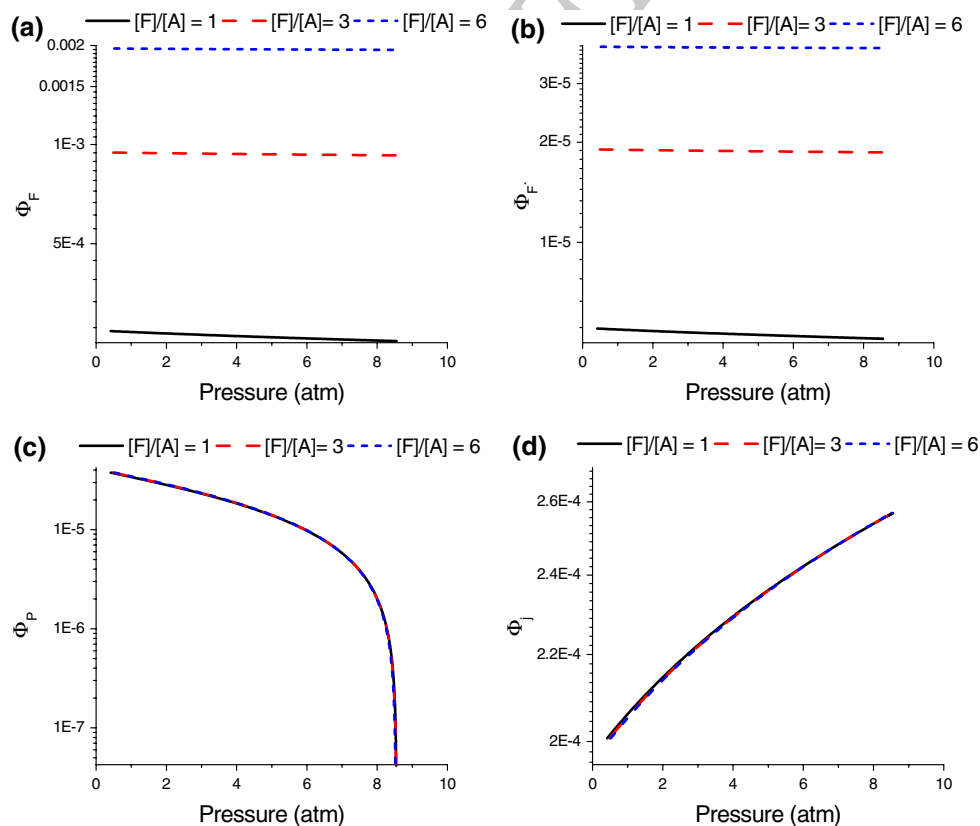


FIGURE 2. Bundle formation is favored at higher thermodynamic pressure and indifferent to different fascin:actin molar ratios. The above graphs show the calculated volume fraction for fascin [ϕ_F , (a)], activated fascin [ϕ_{F^*} , (b)], unreacted F-actin polymer [ϕ_P , (c)], and bundles [ϕ_b , (d)] for different molar fascin:actin ratios and a function of pressure. In the above graphs, a, b, and c are plotted in semi-log form whereas d is in linear scale. The parameters used were: $s_F = 4640$, $s_{F^*} = 4600$, $K_{X\text{-link}} = 2.66 \times 10^8$, $K_{\text{deact}} = 2.66 \times 10^8$, and $[A] = 9.52 \times 10^9$ M.

325 pressure ranging from 1 to 10 atm³). The pressures of
 326 interest were selected between 1 and 10 atmospheres as
 327 this was in the order of the pressure range investigated
 328 using an extended Flory–Huggins type model for actin
 329 polymerization.³ More over, a back of the envelope
 330 calculation which assumed pico-newton forces at the
 331 filopodia of migrating cells showed that this pressure
 332 range was relevant for biological systems.

333 Next, the interaction parameters, χ_{sp} , χ_{sb} , and χ_{sF}
 334 needed to be determined. Unfortunately, no directly
 335 applicable experimentally data existed for us to deter-
 336 mine these interaction parameters. As a result, esti-
 337 mations needed to be made to determine these
 338 parameters with the following constraints. First, Flory–
 339 Huggins theory gives us the functional form of these
 340 interaction parameters to be directly dependent on the
 341 microscopic energy between the two species, ε_{ij} , and
 342 inversely dependent on the thermal energy in the sys-
 343 tem ($k_B T$). Furthermore, we assume that all these
 344 parameter are of the same order of magnitude and that
 345 these interaction parameters satisfied the mathematical
 346 constraints for the exponential “ a .” With these con-
 347 straints in mind, χ_{sp} , χ_{sb} , and χ_{sF} were determined such

that $2*a + b \sim O(-10^0)$. Using the hydrodynamic
 diameter of actin and fascin in solution the numerical
 values for the size constants were defined as follows

$$\begin{aligned} s_p &= 2300 \\ s_{F^*} &= 4600 \\ s_s &= s_v = 1 \end{aligned} \quad (20)$$

This leaves, s_F , s_{x-link} , s_{p^*} to be “user-defined”
 parameters in our model. Based on previous studies of
 actin and to keep the model simple, we assumed that
 $s_{F^*} = s_{x-link}$ and $s_{p^*} = i*s_p$ where i was the extent of
 polymerization of each F-actin polymer.

Finally, for K_{x-link} experimentally determined data
 from *in vivo* experiments³³ were used to define this
 value as 6.7×10^6 . Unfortunately, no explicit data was
 found for K_{deact} , however, as the deactivation of fascin
 is known to be mediated by the phosphorylation of a
 ser-39 amino acid a good starting point for the equi-
 librium was to assume that a full energy transferred
 occurred between the hydrolysis of ATP to ADP and
 to use that free energy (i.e., $\Delta G_{Hydrolysis}$). This gave us a
 starting value for K_{deact} of 2.66×10^8 . This variable

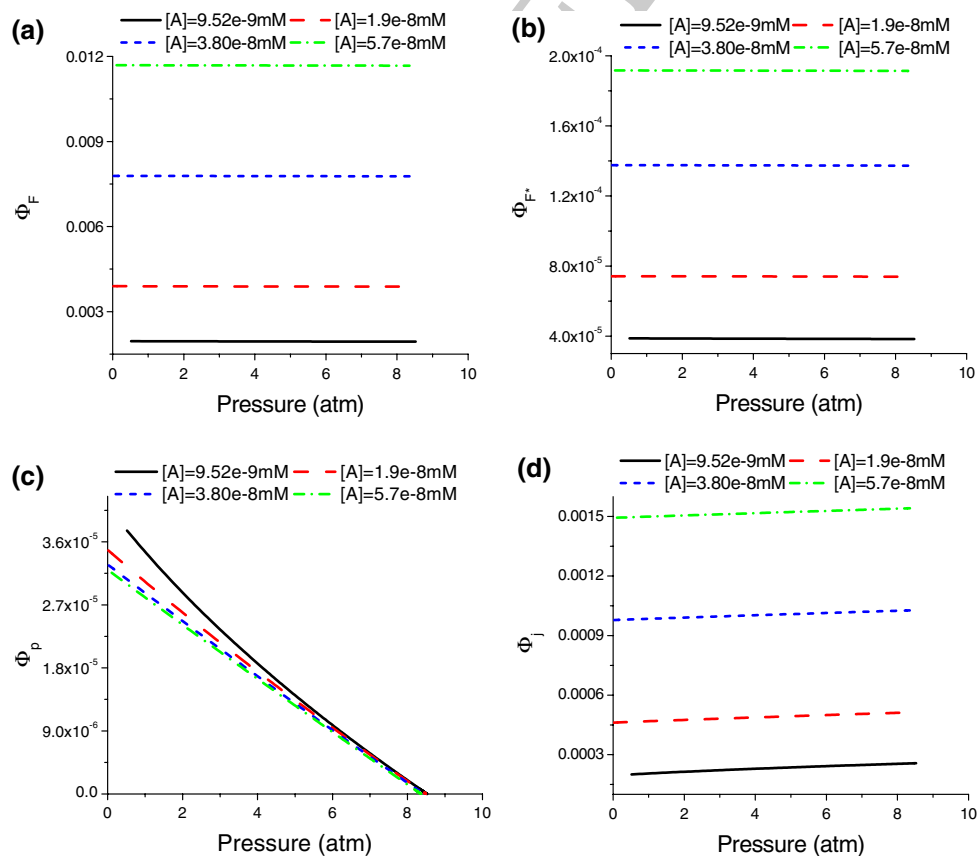


FIGURE 3. F-actin is the limiting reagent in bundle formation. The above graphs show the calculated volume fraction for fascin [ϕ_F , (a)], activated fascin [ϕ_{F^*} , (b)], unreacted F-actin polymer [ϕ_p , (c)], and bundles [ϕ_b , (d)] for different actin concentration keeping fascin:actin ratio constant and as a function of thermodynamic pressure. The parameters used were: $s_F = 4640$, $s_{F^*} = 4600$, $K_{x-link} = 6.7 \times 10^6$, $K_{deact} = 2.66 \times 10^8$, and $[F]/[A] = 6$.

368 was changed up and down two orders of magnitude to
 369 see the dependence of our system on the concentration
 370 of available activated fascin. Finally, an overview of all
 371 parameters with their dimensions and values used in
 372 the numerical calculation can be seen in Table 1.

373 RESULTS AND DISCUSSION

374 Figure 2 shows the results obtained for the system's
 375 composition (i.e., ϕ_p , ϕ_F , ϕ_{F^*} , and ϕ_j) as a function of
 376 thermodynamic pressure. Here three different initial
 377 conditions are plotted on a semi-logarithmic plot to
 378 show the dependence of these curves on the initial actin
 379 to fascin molar ratios. The figure shows that as pres-
 380 sure increases the volume fraction of F-actin and
 381 activated fascin decreases corresponding to an increase
 382 in the total volume fraction consisting of bundles.
 383 Furthermore, upon increasing initial ratios of actin-to-
 384 fascin the deactivated fascin volume fraction increased.
 385 This leads us to conclude that for the conditions used,
 386 our reaction is F-actin limited and not fascin limited.
 387 We also note that the volume fraction of activated
 388 fascin is significantly less than that of the deactivated
 389 fascin. We believe this due to the large equilibrium

constants for both reactions leading to a competition
 between the deactivated fascin and the bundle poly-
 mer. In this plot, the compositions' pressure depen-
 dence is simply due to the multispecies nature of
 reaction two rather than any changes in conformation
 between the reactants and products as the size
 parameters between the products reactants were kept
 constant.

Next we consider the effect of keeping the fascin-to-
 actin ratio constant (i.e., $[F]/[A] = 6$) while varying the
 initial actin concentration. Figure 3 shows the results
 for each of the species involved upon varying the
 concentration from 9.52×10^{-9} to 5.7×10^{-8} mM.
 Again we notice that the system is limited by the actin
 concentration. As expected the concentration of bun-
 dle increases as the actin, and conversely the fascin,
 concentration increase.

Figure 4 shows the dependence of changing the size
 parameter s_F on fascin and deactivated fascin compo-
 sition. Here again, we note that the as one changes the
 size parameter of s_F from being equal to s_{F^*} , equilib-
 rium is pushed toward the activated species at higher
 pressure. Furthermore, in Fig. 4 we fixed the size
 parameter for s_{F^*} to be equal to 4600. This was
 determined by approximating the size of activated

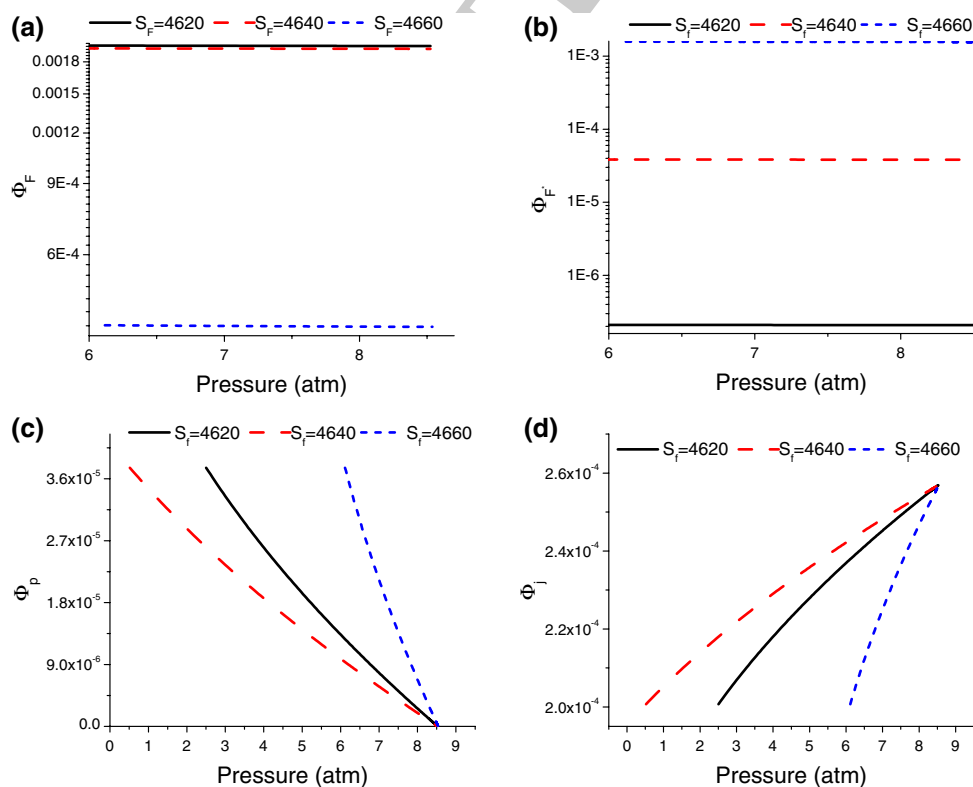


FIGURE 4. Increasing the specific volume of deactivated fascin results in an increase in activated fascin. The above graphs show the calculated species composition for fascin [ϕ_F , (a)], activated fascin [ϕ_{F^*} , (b)], unreacted F-actin polymer [ϕ_p , (c)], and bundles [ϕ_j , (d)] as a function of theoretical pressure and increasing specific volume parameters for deactivated fascin, s_F . The parameters that were kept constant were: $s_{F^*} = 4600$, $K_{x-link} = 6.7 \times 10^6$, $K_{deact} = 2.66 \times 10^8$, $[F]/[A] = 6$, and $[A] = 9.52 \times 10^{-9}$ mM.

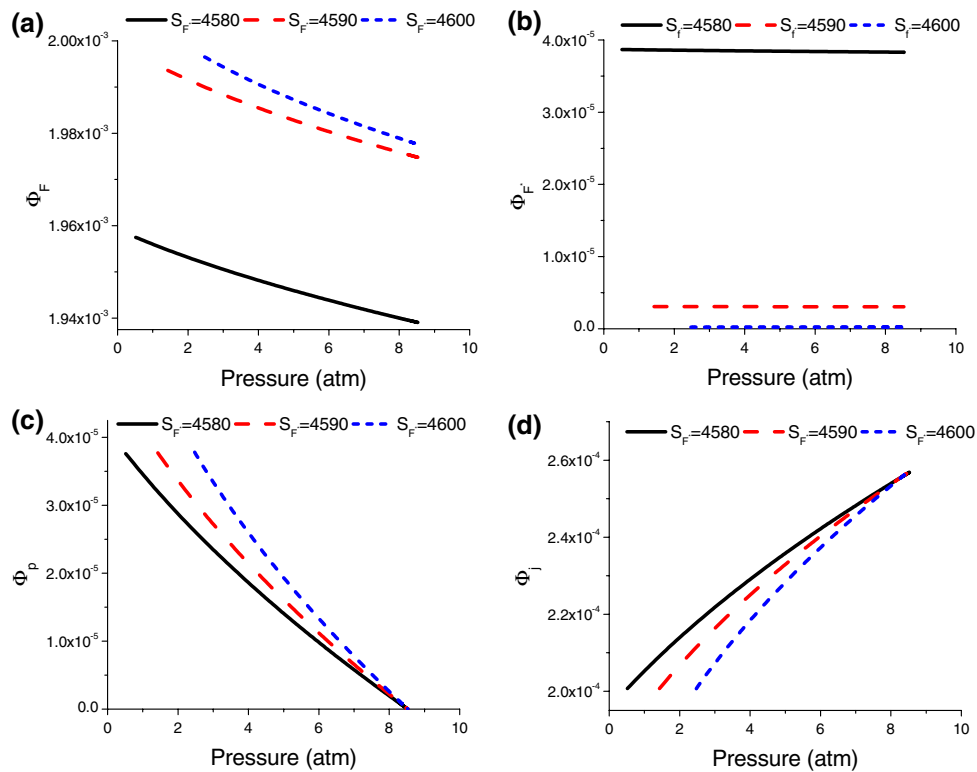


FIGURE 5. Increasing the specific volume of the activated fascin results in a decrease in both activated fascin and bundle volume fractions. The above graphs show the calculated species composition for fascin [ϕ_F , (a)], activated fascin [ϕ_{F^*} , (b)], unreacted F-actin polymer [ϕ_P , (c)], and bundles [ϕ_B , (d)] as a function of thermodynamic pressure and increasing specific volume parameters for activated fascin, s_{F^*} . The parameters that were kept constant were: $s_F = 4640$, $K_{x-link} = 6.7 \times 10^6$, $K_{deact} = 2.66 \times 10^8$, $[F]/[A] = 6$, and $[A] = 9.52 \times 10^{-9}$ mM.

415 fascin from experimental data in physiological condi- 440
 416 tions. However, as this was an approximated value we 441
 417 were interested in seeing how the system responded to 442
 418 perturbations around this value while keeping s_F con- 443
 419 stant at 4640. Figure 5 shows how our system 444
 420 responded to these perturbations. We noticed that with 445
 421 increasing s_{F^*} concentrations a corresponding decrease 446
 422 in unreacted polymer and increase in bundle compo- 447
 423 sition occurs (c, d). Both of these trends are consistent 448
 424 with our results from Figs. 2 and 3 showing that actin 449
 425 is the limiting reactant for bundle formation for an 450
 426 actin:fascin molar ratio of 1:6. 451

427 We note that in Figs. 4 and 5 the dependence of the 452
 428 unreacted polymer and bundle on s_F and s_{F^*} is dif- 453
 429 ferent. We hypothesized that this was due to a mini- 454
 430 mum in the system's free energy occurring around the 455
 431 $s_F \sim 4645$ whereas the free energy reaches no such 456
 432 minimum for the range of s_{F^*} selected. To test this 457
 433 hypothesis the free energy was plotted against s_F and 458
 434 s_{F^*} over the range of interest (Fig. 6) and a minimum 459
 435 was observed for s_F but not for s_{F^*} . Since systems will 460
 436 tend to minima in free energy, the our results suggest 461
 437 that $s_F \sim 4640$ is the optimal value for this parameter.

438 Finally, Fig. 7 shows the dependence of changing 462
 439 the K_{deact} on the system composition. For clarity, we

only report results of unreacted F-actin and bundle 440
 compositions, as other results are qualitatively similar. 441
 Our results shows that by changing K_{deact} one can 442
 predict the dependence of the initiation of bundle 443
 formation has on pressure. Moreover, this figure is 444
 consistent with the experimental data showing that the 445
 deactivation of fascin is regulated by the phosphory- 446
 lation of the ser39 amino acid. Thus we observe that in 447
 order for bundles to form at atmosphere K_{deact} must be 448
 equal to 2.66×10^8 . This value calculated from 449
 the hydrolysis of ATP at physiological conditions 450
 (i.e., 1 atm) and as such confirms aforementioned 451
 experiments. 452

DISCUSSION AND CONCLUSION 453

While our model is able to capture a number of key 454
 processes in fascin crosslinking, accurate comparison 455
 with experiment was difficult due to lack of reliable 456
in vitro or *in vivo* experimental data. As a result, a 457
 number of parameters had to be approximated, mak- 458
 ing our results qualitative. Nonetheless, ours is the first 459
 attempt of its kind, rooted in first principles, to include 460
 fascin structure, chemical and mechanical properties in 461

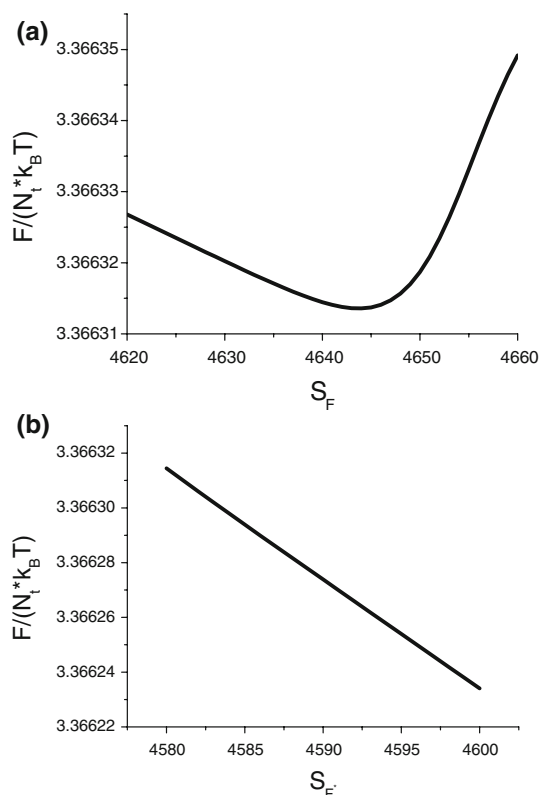


FIGURE 6. An optimal value for s_F exists at a free energy minimum whereas no such free energy minimum occurs for s_{F^*} . In the above graph the derived Helmholtz free energy normalized for thermal energy is plotted against both volume size parameters for deactivated [s_F , (a)] and activated [s_{F^*} , (b)]. A local minimum in free energy at $s_F = 4645$ suggest an optimal value for the deactivated fascin volume size parameter. No such minimum exist in b explaining the difference in the subplots for ϕ_P and ϕ_j in Figs. 4 and 5. The parameters that were kept constant were: $s_{F^*} = 4600$ (a), $s_F = 4640$ (b), $K_{x-link} = 6.7 \times 10^6$, $K_{deact} = 2.66 \times 10^8$, $[F]/[A] = 6$, and $[A] = 9.52 \times 10^{-9}$ mM.

462 a model of actin-fascin bundle formation. Our model
 463 predicts that the formation of bundles is F-actin lim-
 464 ited and becomes more favorable upon increase in
 465 thermodynamic pressure. It also predicts a theoretical
 466 value for the size of deactivated fascin in aqueous
 467 solutions. Both of these predictions can be tested and
 468 refined with future experiments. The prediction made
 469 by our model with regards to the bundle formation's
 470 extent of reaction dependence on thermodynamic
 471 pressure can be tested in an *in situ* fashion similar to
 472 that used by Artyomov *et al.* Using this experimental
 473 data, the size parameter can be further refined such
 474 that the trend observed in experiments match our
 475 theory. This refined size parameter for deactivated
 476 fascin can then be tested using Small Angle Neutron
 477 Scattering (SANS) similar to what has been previously
 478 done²⁵ for other biological systems. In general, this
 479 model gives us a better understanding of how
 480 fascin:actin bundles develop under pressure and may

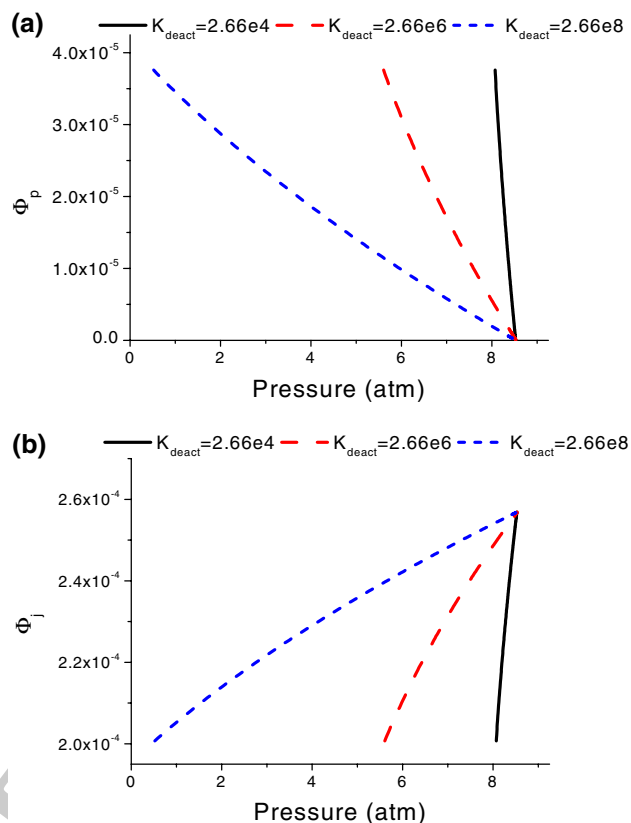


FIGURE 7. K_{deact} determines the pressure upon bundle initiation. The graphs show the dependence of the volume fraction for unreacted F-actin polymer [ϕ_P , (a)] and bundles [ϕ_j , (b)] as a function of pressure for different K_{deact} . The K_{deact} determined from the full energy transfer of the hydrolysis of ATP to ADP was equal to 2.66×10^8 . This graph is consistent with the experiments showing that deactivation of fascin is mediated by the phosphorylation of the ser39 amino acid as bundle formation at atmospheric pressure only occurs for the K_{deact} equal to 2.66×10^8 . The parameters that were kept constant were: $s_{F^*} = 4600$, $s_F = 4640$, $K_{x-link} = 6.7 \times 10^6$, $[F]/[A] = 6$, and $[A] = 9.52 \times 10^{-9}$ mM.

lead to development of improved cell physiological
 models describing how cells interact with their sub-
 strates as they grow and migrate on complex natural
 and synthetic environments. How great of an impact
 depends on whether a better understanding of func-
 tionalized images of actin bundling formation in live
 migrating cells can be achieved.

ACKNOWLEDGMENTS

MHZ gratefully acknowledges the support of
 Robert A. Welch Foundation (Grant # F-1677). We
 are also grateful to Prof. Karl Freed for his feedback
 and insightful comments on various stages of the
 model development. Members of our lab, particularly
 Tianyi Yang, are gratefully acknowledged for their
 feedback.

- 498 ¹Aratyn, Y. S., T. E. Schaus, E. W. Taylor, and G. G. 559
 499 Borisov. Intrinsic dynamic behavior of fascin in filopodia. 560
 500 *Mol. Biol. Cell* 18(10):3928–3940, 2007. 561
 501 ²Artyomov, M. N., and K. F. Freed. Compressible models of 562
 502 equilibrium polymerization. *J. Chem. Phys.* 123(19), 2005. 563
 503 ³Artyomov, M. N., and K. F. Freed. Actin polymerization 564
 504 under pressure: a theoretical study. *J. Chem. Phys.* 126(2), 565
 505 2007. 566
 506 ⁴Bentley, D., and A. Torioian-Raymond. Disoriented path- 567
 507 finding by pioneer neurone growth cones deprived of filopodia 568
 508 by cytochalasin treatment. *Nature* 323(6090):712–715, 1986. 569
 509 ⁵Bershadsky, A. D., N. Q. Balaban, and B. Geiger. Adhesion- 570
 510 dependent cell mechanosensitivity. *Annu. Rev. Cell Dev. 571*
 511 *Biol.* 19:677–695, 2003. 572
 512 ⁶Clark, P., P. Connolly, A. S. Curtis, J. A. Dow, and C. D. 573
 513 Wilkinson. Topographical control of cell behaviour. I. 574
 514 Simple step cues. *Development* 99(3):439–448, 1987. 575
 515 ⁷den Braber, E. T., J. E. de Ruijter, H. T. Smits, L. A. 576
 516 Ginsel, A. F. von Recum, and J. A. Jansen. Effect of 577
 517 parallel surface microgrooves and surface energy on cell 578
 518 growth. *J. Biomed. Mater. Res.* 29(4):511–518, 1995. 579
 519 ⁸Dowell-Mesfin, N. M., M. A. Abdul-Karim, A. M. Turner, 580
 520 S. Schanz, H. G. Craighead, B. Roysam, J. N. Turner, and 581
 521 W. Shain. Topographically modified surfaces affect orienta- 582
 522 tion and growth of hippocampal neurons. *J. Neural Eng.* 583
 523 1(2):78–90, 2004. 584
 524 ⁹Dudowicz, J., K. F. Freed, and J. F. Douglas. Lattice 585
 525 model of living polymerization. I. Basic thermodynamic 586
 526 properties. *J. Chem. Phys.* 111(15):7116–7130, 1999. 587
 527 ¹⁰Dudowicz, J., K. F. Freed, and J. F. Douglas. Lattice 588
 528 model of living polymerization. II. Interplay between 589
 529 polymerization and phase stability. *J. Chem. Phys.* 590
 530 112(2):1002–1010, 2000. 591
 531 ¹¹Dudowicz, J., K. F. Freed, and J. F. Douglas. Lattice 592
 532 model of living polymerization. III. Evidence for particle 593
 533 clustering from phase separation properties and “round- 594
 534 ing” of the dynamical clustering transition. *J. Chem. Phys.* 595
 535 113(1):434–445, 2000. 596
 536 ¹²Dudowicz, J., K. F. Freed, and J. F. Douglas. Lattice 597
 537 model of equilibrium polymerization. IV. Influence of 598
 538 activation, chemical initiation, chain scission and fusion, 599
 539 and chain stiffness on polymerization and phase separa- 600
 540 tion. *J. Chem. Phys.* 119(23):12645–12666, 2003. 601
 541 ¹³Fallon, J. R. Neurite guidance by non-neuronal cells in 602
 542 culture: preferential outgrowth of peripheral neurites on 603
 543 glial as compared to nonglial cell surfaces. *J. Neurosci.* 604
 544 5(12):3169–3177, 1985. 605
 545 ¹⁴Foley, J. D., E. W. Grunwald, P. F. Nealey, and C. J. 606
 546 Murphy. Cooperative modulation of neuritogenesis by 607
 547 PC12 cells by topography and nerve growth factor. *Bio-* 608
 548 *materials* 26(17):3639–3644, 2005. 609
 549 ¹⁵Forciniti, L., C. E. Schmidt, and M. H. Zaman. Compu- 610
 550 tational model provides insight into the distinct responses 611
 551 of neurons to chemical and topographical cues. *Ann. Bio-* 612
 552 *med. Eng.* 2008. 613
 553 ¹⁶Geiger, B., and A. Bershadsky. Assembly and mechano- 614
 554 sensory function of focal contacts. *Curr. Opin. Cell Biol.* 615
 555 13(5):584–592, 2001. 616
 556 ¹⁷Geiger, B., and A. Bershadsky. Exploring the neighbor- 617
 557 hood: adhesion-coupled cell mechanosensors. *Cell* 110(2): 618
 558 139–142, 2002. 619
 620
 621
 622
 623
 624
 625
 626
 627
 628
 629
 630
 631
 632
 633
 634
 635
 636
 637
 638
 639
 640
 641
 642
 643
 644
 645
 646
 647
 648
 649
 650
 651
 652
 653
 654
 655
 656
 657
 658
 659
 660
 661
 662
 663
 664
 665
 666
 667
 668
 669
 670
 671
 672
 673
 674
 675
 676
 677
 678
 679
 680
 681
 682
 683
 684
 685
 686
 687
 688
 689
 690
 691
 692
 693
 694
 695
 696
 697
 698
 699
 700
 701
 702
 703
 704
 705
 706
 707
 708
 709
 710
 711
 712
 713
 714
 715
 716
 717
 718
 719
 720
 721
 722
 723
 724
 725
 726
 727
 728
 729
 730
 731
 732
 733
 734
 735
 736
 737
 738
 739
 740
 741
 742
 743
 744
 745
 746
 747
 748
 749
 750
 751
 752
 753
 754
 755
 756
 757
 758
 759
 760
 761
 762
 763
 764
 765
 766
 767
 768
 769
 770
 771
 772
 773
 774
 775
 776
 777
 778
 779
 780
 781
 782
 783
 784
 785
 786
 787
 788
 789
 790
 791
 792
 793
 794
 795
 796
 797
 798
 799
 800
 801
 802
 803
 804
 805
 806
 807
 808
 809
 810
 811
 812
 813
 814
 815
 816
 817
 818
 819
 820
 821
 822
 823
 824
 825
 826
 827
 828
 829
 830
 831
 832
 833
 834
 835
 836
 837
 838
 839
 840
 841
 842
 843
 844
 845
 846
 847
 848
 849
 850
 851
 852
 853
 854
 855
 856
 857
 858
 859
 860
 861
 862
 863
 864
 865
 866
 867
 868
 869
 870
 871
 872
 873
 874
 875
 876
 877
 878
 879
 880
 881
 882
 883
 884
 885
 886
 887
 888
 889
 890
 891
 892
 893
 894
 895
 896
 897
 898
 899
 900
 901
 902
 903
 904
 905
 906
 907
 908
 909
 910
 911
 912
 913
 914
 915
 916
 917
 918
 919
 920
 921
 922
 923
 924
 925
 926
 927
 928
 929
 930
 931
 932
 933
 934
 935
 936
 937
 938
 939
 940
 941
 942
 943
 944
 945
 946
 947
 948
 949
 950
 951
 952
 953
 954
 955
 956
 957
 958
 959
 960
 961
 962
 963
 964
 965
 966
 967
 968
 969
 970
 971
 972
 973
 974
 975
 976
 977
 978
 979
 980
 981
 982
 983
 984
 985
 986
 987
 988
 989
 990
 991
 992
 993
 994
 995
 996
 997
 998
 999
 1000